

UWB Indoor Global Localisation for Nonholonomic Robots with Unknown Offset Compensation

Daniele Fontanelli¹, Farhad Shamsfakhr¹, Paolo Bevilacqua² and Luigi Palopoli²

Abstract—The problem addressed in this paper is the localisation of a mobile robot using a combination of on-board sensors and Ultra-Wideband (UWB) beacons. Specifically, we consider a scenario in which a mobile robot travels across an area infrastructured with a small number of UWB anchors. The presence of obstacles in the environment introduces an offset in the measurements of the distance between the robot and the UWB anchors causing a degradation in the localisation performance. By using a discrete-time formulation of the system dynamics, we show that, under mild condition, the trajectories can be observed and the offset can be estimated in a finite number of steps. Besides being interesting in its on right, the global observability results offer a clear pathway towards the definition of a new generation of estimation algorithms.

I. INTRODUCTION

An accurate localisation is the mainstay of the vast majority of mobile robot applications [1]. When a robot's task is mission critical and/or the robot travels across spaces shared with humans, a customary requirement is imposing an uncertainty in the order of a few centimetres for the planar positioning and of a few degrees (or of fractions of degrees) for the orientation. These requirements are far from easy to meet in indoor environments, where the Global Positioning System (GPS) signals are blocked or attenuated by the walls. For this reason, several solutions have been proposed in the past few years. In this paper, we will discuss how to solve the problem by using a small number of Ultra-Wideband beacons in the presence of obstructions.

A. Related Work

Classical approaches for indoor localisation of robots. The use of reflexive markers is the localisation solution adopted by Laser Guided Vehicles, but it requires a heavy infrastructure, which is very expensive to deploy and maintain. At the opposite end of the spectrum are infrastructure-free solutions, such as using Light Detection and Ranging (LiDAR) sensors [2], or visual SLAM [3], [4]. Visual SLAM is certainly the promised land of robot localisation, but when the environment is highly dynamic its reliability and its robustness become questionable [5]. An obvious possibility for vision-based localisation is to support SLAM techniques by the use of markers located at known positions [6] or deployed on purpose [7], [8]. Visual markers can only be used in Line of Sight (LOS) conditions, require a proper illumination and the availability of an adequate computing power on board. A different possibility is to use multilateration solutions that

exploit the distance measured from a set of wireless nodes (frequently referred to as *anchors*). The distance from each anchor node can be estimated indirectly from the Received Signal Strength Indication (RSSI) values [9], [10] or from the Time-of-Arrival (ToA), the Time-Difference-of-Arrival (TDoA) or Round-Trip Time (RTT) of messages exchanged between each anchor node and the wireless transceiver installed on the robot. The adoption of these techniques have been plagued by the presence of different detrimental effects that significantly reduces the accuracy of the measurements. **The new frontier of UWB localisation.** The use of Ultra-Wideband signals [11] promises to be a solution to these problems. The key advantage of UWB-based ranging is that the wide bandwidth enables to measure ToA and RTT with a much higher precision than by using other wireless technologies [12]. As a result, the uncertainty associated with distance measurements is in the order of a few centimetres. Moreover, the recent availability of new-generation smaller and low-cost transceivers offering decimeter-level accuracy (e.g., the DecaWave DW1000 [13]) has lowered the adoption barriers for this technology. The availability of low cost platforms has sparked an enthusiastic interest for this type of localisation technologies in robotics. The results are particularly exciting when UWB anchors are used in combination with dead-reckoning technologies (e.g., wheel encoders, IMU). By using standard sensor fusion techniques, several authors report localisation errors in the order of a few tens of centimetres for the planar positioning and of a few degrees for the angular error [14]–[16].

Obstructions and sparse infrastructures. In order to make UWB a practically viable solution for robot localisation, at least two problems need to be addressed. The first is how many anchors are needed for a reliable localisation? An equivalent reformulation is to understand if it is possible to localise a robot using a sparse infrastructure. This question is obviously motivated by the cost of the infrastructure or by the objective difficulty of deploying many nodes in specific areas or environments. The second problem is if it is possible to make a localisation system reliable in presence of obstructions between the anchors and the robot. When a measurement is collected in Non Line Of Site (NLOS) conditions the distance measurements get affected by an unknown offset and the resulting performance of standard algorithms significantly degrades [17].

UWB localisation with a small number of anchors has been addressed in our previous work [18], [19], from the perspective of the global observability of the robot's trajectories. Specifically, we have shown that three anchors are always

¹ Dept. of Industrial Engineering, University of Trento, Trento, Italy.

² Dept. of Engineering and Computer Science, University of Trento, Trento, Italy.

sufficient for global state reconstruction, while two are not if the robot moves on a straight line. A probabilistic approach to the problem of localisation in presence of occlusions has been proposed by Prorok et al. [20], who proposes a collaborative localisation approach for a set of robots that integrates the knowledge of LOS/NLOS condition.

B. Paper contribution

The work in this paper is motivated by two important considerations. First, the two problems of localisation using a sparse infrastructure (i.e., a small number of anchors) and of localisation in NLOS conditions are actually intertwined. Indeed, if we use a large number of anchors the problem of NLOS conditions can be alleviated by using robust regression [21]. On the contrary, when the visible anchors are in a small number, we cannot afford discarding any measurement, even if it is affected by an unknown offset. Our second observation is that it is almost impossible for a robot to know whether or not it is in LOS conditions from an anchor if it is not localised (which is the problem we want to solve). So, the presence of offsets should be inferred only from the distance measurements.

Motivated by these considerations, we present a global observability analysis for a robot localising itself by merging proprioceptive data from its onboard sensors with external measurements from a number of UWB anchors that are not required to be in LOS conditions. Through a few algebraic manipulations of the robot discrete-time dynamics, we construct an observer based on a set of linear equations that produce the orientation of the robot and the value of the offsets under a set of mild conditions on the number of anchors (at least two are required), on the trajectory of the robot (it has to make some turn if we use only two anchors), and on the changes in the distance offset (they have to remain constant for a limited number of samples to give the observer enough information to converge). Motivated by this analysis, we also propose the application of standard Extended Kalman Filter (EKF), and show its efficacy in our simulation scenarios.

The rest of this manuscript is structured as follows. Section II presents the models adopted and the problem we are aiming at. The global observability analysis underlying the formulation of the positioning problem is offered in Section III. Extensive simulation results are reported in Section IV in order to confirm the validity and the good performances of the proposed approach. Section V reports some experimental results collected on the field and, finally, in Section VI conclusions and the future work directions are outlined.

II. BACKGROUND AND PROBLEM FORMULATION

Robot model. Consider a unicycle-like robot moving according to the following kinematic model

$$\begin{bmatrix} \dot{x} \\ \dot{y} \\ \dot{\theta} \end{bmatrix} = \begin{bmatrix} v \cos \theta \\ v \sin \theta \\ \omega \end{bmatrix}, \quad (1)$$

where $s(t) = [x, y, \theta]^T$ is the state of the system, θ is the orientation of the vehicle with respect to axis X_w of a reference frame $\langle W \rangle$, v is the robot forward velocity and ω is the robot angular velocity. As discussed in [18], [19], assuming that during the sampling period T_s the velocities v and ω are held constant and denoting with $s((k+1)T_s) = s_{k+1} = [x_{k+1}, y_{k+1}, \theta_{k+1}]^T$, it is possible to find the following discrete-time equivalent dynamics for (1), i.e.

$$\begin{aligned} x_{k+1} &= x_k + \Phi_k \cos(\theta_k) - \Psi_k \sin(\theta_k) = x_k + f_{x_k}, \\ y_{k+1} &= y_k + \Psi_k \cos(\theta_k) + \Phi_k \sin(\theta_k) = y_k + f_{y_k}, \\ \theta_{k+1} &= \theta_k + 2\phi_k, \end{aligned} \quad (2)$$

where $\Phi_k = A_k \cos(\phi_k)$, $\Psi_k = A_k \sin(\phi_k)$, $\phi_k = \frac{\omega_k}{2} T_s$ and $A_k = 2 \frac{v_k}{\omega_k} \sin(\frac{\omega_k}{2} T_s)$. Moreover, we notice that when $\omega_k \rightarrow 0$, we have

$$\lim_{\omega_k \rightarrow 0} A_k = \lim_{\omega_k \rightarrow 0} 2 \frac{v_k}{\omega_k} \sin\left(\frac{\omega_k}{2} T_s\right) = v_k T_s.$$

Finally, for the sake of brevity, the following symbols \mathbb{S}_k and \mathbb{T}_k will be used to denote if, at time step k , the robot moves straight (i.e., $\omega_k = 0$) or if it moves along a curvilinear path (i.e., $\omega_k \neq 0$), respectively. We assume that the robot inputs (v_k, ω_k) are available by means of, e.g., encoders on the wheels sampled with T_s .

UWB ranging using ToA The vehicle moves across a space instrumented with m UWB anchor nodes. The range measurements from the anchors are taken using time-of-arrival (TOA). TOA is the one-way or two-way propagation time of the radio frequency signal emitted by a source at time t_0 and received by a destination node at time $t_1 = t_0 + \tau$. Let $\bar{z}_{i,k}$ be the distance between the source (i.e., the UWB emitter on the robot) and the i -th destination node at time kT_s , with $k \in \mathbb{N}$ and with T_s being the ranging system sampling time. Let the anchors have coordinates (X_i, Y_i) in the frame $\langle W \rangle$. This quantity is obtained by multiplying the propagation time τ by the propagation speed c :

$$\bar{z}_{i,k} = c\tau_{i,k} = c(t_1 - t_0) = \sqrt{(X_i - x_k)^2 + (Y_i - y_k)^2}, \quad (3)$$

Due to timestamp and time synchronisation uncertainties between the emitting and the receiving nodes, the ranging measurements are affected by an uncorrelated, zero-mean and white Gaussian random noise $\epsilon_{i,k}$ that is responsible of the ranging uncertainty, i.e. $z_{i,k} = \bar{z}_{i,k} + \epsilon_{i,k}$. In addition, the presence of static and dynamic obstacles, e.g. walls and human beings or other robots, generates non line of sight (NLOS) conditions, which determine signal attenuation. As a result, the actual measured distance $z_{i,k}$ is further affected by the presence on an unknown offset $o_{i,k}$, i.e.

$$z_{i,k} = \bar{z}_{i,k} + o_{i,k} + \epsilon_{i,k}, \quad (4)$$

where $o_{i,k} > 0$ by definition, i.e. the propagation time may only increase due to the presence of obstacles.

Problem formulation The problem addressed in this paper is described in the following terms. Consider a robot moving with the dynamics (2). Suppose that the robot starts from

an unknown initial configuration s_0 , that the robot collects distance measurements for the anchors located at (X_i, Y_i) affected by an unknown but constant offset $o_{i,k}$. Our objectives are two fold: 1. finding the conditions under which the initial position and the offsets can be estimated in a finite number of steps, 2. showing a filter that is able to estimate these quantities.

III. OBSERVABILITY ANALYSIS

As discussed in [18], the system is globally observable when offsets are zero, as reported in the following theorems.

Theorem 1 ([18]): Consider a robot with kinematic (2), output function (3), $m = 2$ ranging sensors that moves with non-null forward velocity $v_k \neq 0$. Then:

- If the system follows rectilinear trajectories (i.e., $\mathbb{S}_k, \forall k$), then its state is not globally observable;
- If the system turns twice in a row (e.g. $\mathbb{T}_0\mathbb{T}_1$) then its state is globally observable if $\omega_0 T_s \neq l\pi$, and $\omega_1 T_s \neq l\pi$, for $l \in \mathbb{N}$.

Trivially, the use of $m \geq 3$ non-collinear anchor nodes avoids any ambiguity in estimating any trajectory with $v_k \neq 0$, thus enabling global observability if trilateration or multilateration from the anchors is applied twice in a row when the robot is in two different nearby positions [18].

To prove that it is actually possible to estimate the offsets from the measurements (4), we first compute $z_{i,k}^2 = \bar{z}_{i,k}^2 + o_{i,k}^2 + 2\bar{z}_{i,k}o_{i,k}$, where we have considered the uncertainty $\epsilon_{i,k} = 0$ as customary for any observability analysis. Since from (3) we can derive that

$$\bar{z}_{i,k}^2 - \bar{z}_{j,k}^2 = \Delta_{X_{ij}} + \Delta_{Y_{ij}} + 2 \begin{bmatrix} \delta_{X_{ji}} & \delta_{Y_{ji}} \end{bmatrix} \begin{bmatrix} x_k \\ y_k \end{bmatrix},$$

where $\Delta_{X_{ij}} = X_i^2 - X_j^2$, $\Delta_{Y_{ij}} = Y_i^2 - Y_j^2$, $\delta_{X_{ji}} = X_j - X_i$ and $\delta_{Y_{ji}} = Y_j - Y_i$, we have that once applied to (4) this yields to

$$\Delta_{z_{ij,k}} = z_{i,k}^2 - z_{j,k}^2 = \Delta_{X_{ij}} + \Delta_{Y_{ij}} + 2 \begin{bmatrix} \delta_{X_{ji}} & \delta_{Y_{ji}} \end{bmatrix} \begin{bmatrix} x_k \\ y_k \end{bmatrix} + o_{i,k}^2 - o_{j,k}^2 + 2(\bar{z}_{i,k}o_{i,k} - \bar{z}_{j,k}o_{j,k}).$$

As a consequence, provided that $o_{i,k} = o_{i,k+1}$, $\forall i = 1, \dots, m$, it follows that

$$\Delta_{ij}^{k+1} = \Delta_{z_{ij,k+1}} - \Delta_{z_{ij,k}} = 2 \begin{bmatrix} \delta_{X_{ji}} & \delta_{Y_{ji}} \end{bmatrix} \begin{bmatrix} f_{x_k} \\ f_{y_k} \end{bmatrix} + 2(\delta_{\bar{z}_{i,k+1}}o_{i,k} - \delta_{\bar{z}_{j,k+1}}o_{j,k}), \quad (5)$$

where the presence of $[f_{x_k}, f_{y_k}]^T$ comes from the first two equations of (2) and $\delta_{\bar{z}_{i,k+1}} = \bar{z}_{i,k+1} - \bar{z}_{i,k}$. A few remarks are now in order. First, $\delta_{\bar{z}_{i,k+1}} = z_{i,k+1} - z_{i,k} = \delta_{z_{i,k+1}}$. Second, the unknowns in (5) f_{x_k} , f_{y_k} and $o_{i,k}$, $\forall i = 1, \dots, m$, are linearly related to the other quantities and, since the unknowns involve the state variable θ_k embedded in f_{x_k} and f_{y_k} , the possibility to reconstruct the offsets has to be carried out together with the robot observability. Third, $\Delta_{jl}^{k+1} = \Delta_{il}^{k+1} - \Delta_{ij}^{k+1}$, $\forall i, j, l$. As a consequence, from m anchors and two time instants $(k+1)T_s$ and kT_s , we can collect at most $m-1$ linearly independent relations (5)

(expressed, without loss of generality, with respect to $i = 1$) in $m+2$ unknowns.

If we consider two additional time instants, namely $(k+2)T_s$ and $(k+1)T_s$ in (5), we can collect $m-1$ additionally linearly independent relations. The main problem is that Δ_{ij}^{k+2} will be a function of the same offsets $o_{i,k}$, $\forall i = 1, \dots, m$, but also of $f_{x_{k+1}}$, $f_{y_{k+1}}$. However, considering (2), we can define the following recursive formula

$$S_{k+1} = \frac{1}{A_k} \begin{bmatrix} \Phi_{k+1} & -\Psi_{k+1} \\ \Psi_{k+1} & \Phi_{k+1} \end{bmatrix} \begin{bmatrix} \cos(\phi_k) & -\sin(\phi_k) \\ \sin(\phi_k) & \cos(\phi_k) \end{bmatrix} S_k,$$

with initial condition $S_k = I_2$, which allows us to express

$$\begin{bmatrix} f_{x_{k+1}} \\ f_{y_{k+1}} \end{bmatrix} = S_{k+1} \begin{bmatrix} f_{x_k} \\ f_{y_k} \end{bmatrix},$$

which is a function of the known inputs to the system. Hence, the two additional relations at time instants $(k+2)T_s$ and $(k+1)T_s$ of (5) are indeed a function of the same unknowns, i.e. f_{x_k} , f_{y_k} and $o_{i,k}$, $\forall i = 1, \dots, m$. The previous relation can be further extended using the property of the composition of rotation matrices, thus having

$$\begin{bmatrix} f_{x_{k+n}} \\ f_{y_{k+n}} \end{bmatrix} = S_{k+n} \begin{bmatrix} f_{x_k} \\ f_{y_k} \end{bmatrix} = \frac{A_{k+n}}{A_k} R \left(\sum_{i=0}^n \phi_{k+i} + \sum_{i=1}^{n-1} \phi_{k+i} \right) \begin{bmatrix} f_{x_k} \\ f_{y_k} \end{bmatrix}, \quad (6)$$

which holds true for any $n \geq 1$ and where $R(\alpha)$ is the planar rotation matrix of angle α . Therefore, considering all the time steps k to $k+n$ for (5), we will have $n(m-1)$ relations in $m+2$ unknowns, i.e., the m offsets and the robot motions f_{x_k} , f_{y_k} at time k . It is worthwhile to note that S_{k+n} only comprises the known robot linear and angular velocities and that f_{x_k} and f_{y_k} both depends only on the robot orientation θ_k , hence the unknowns are actually $m+1$. However, explicitly write the problem in terms of θ_k would loose the linearity property, which is a fundamental condition as detailed next.

To show the global observability with m anchors, we first define $h_k = [\Delta_{12}^k \dots \Delta_{1m}^k]^T$, so as to have for n steps $h = [h_{k+1}^T \dots h_{k+n}^T]^T$. Then, we further define $\delta^k = \delta_{z_{1,k}} \mathbf{1}_m$, where $\mathbf{1}_m$ is a column vector filled with m ones, and the diagonal matrix $D^k = \text{diag}(\delta_{z_{2,k}}, \dots, \delta_{z_{m,k}})$, with entries given by of the range differences (except for the chosen reference anchor 1, reported in δ^k). We finally define the matrix

$$B = \begin{bmatrix} \delta_{X_{21}} & \delta_{Y_{21}} \\ \delta_{X_{31}} & \delta_{Y_{31}} \\ \vdots & \vdots \\ \delta_{X_{m1}} & \delta_{Y_{m1}} \end{bmatrix}. \quad (7)$$

As a consequence of these choices, we can construct the following matrix

$$G = \begin{bmatrix} \delta^{k+1} & -D^{k+1} & B \\ \delta^{k+2} & -D^{k+2} & BS_{k+1} \\ \vdots & \vdots & \vdots \\ \delta^{k+n} & -D^{k+n} & BS_{k+n-1} \end{bmatrix}, \quad (8)$$

that finally yields

$$h = 2G \begin{bmatrix} o_k \\ f_{x_k} \\ f_{y_k} \end{bmatrix}, \quad (9)$$

which is the juxtaposition of the relations (5), considering m anchors, n steps and assuming that $o_k = [o_{1,k}, o_{2,k}, \dots, o_{m,k}]^T$. With the presented formulation, the following theorem holds. The proof relies on the invertibility of the matrix G .

Theorem 2: Given a time reference kT_s , n robot inputs (v_{k+l}, ω_{k+l}) , $l = 0, \dots, n-1$, and nm , with $m \geq 2$, range readings $z_{i,k+l}$ with offsets defined in (4), with $i = 1, \dots, m$ and $l = 0, \dots, n-1$, the problem is globally observable w.r.t. o_k , f_{x_k} and f_{y_k} if the following both holds:

- 1) $n \geq \underline{n} = \lceil \frac{m+2}{m-1} \rceil$ and $v_{k+l}, l = 0, \dots, n-1$, not equal to zero for at least \underline{n} times;
- 2) For $m = 2$ anchors, at least 1 turn is needed, e.g. for $l = 0, \dots, n-1$, there exists one time instant $k+l$ such that $\omega_{k+l}T_s \neq l\pi$, for $l \in \mathbb{N}$. Otherwise, $m \geq 3$ non-collinear anchors are needed.

Proof: The value \underline{n} in Condition 1 determines the minimum number of independent rows in G . Instead, if $v_{k+l} = 0$ (namely $A_k = 0$), we have that $\delta_{z_{i,k+l+1}} = 0, \forall i = 1, \dots, m$. Therefore, Condition 1 is a necessary condition to have G column full rank.

The special case of $m = 2$ anchors requires that the robot does not entirely move along a straight path. Indeed, in such a case, all the $\phi_{k+l} = 0, \forall l$, which implies that all the transformation matrices S_{k+l} in (6) will be equal to identity matrices scaled by a factor A_{k+l}/A_k . For the case of $m = 2$ anchors let us assume, without loss of generality, that the two anchors lay on the Y_w axis of the reference frame $\langle W \rangle$. In such a case, the first column of B in (7) will be null. This condition together with $\phi_{k+l} = 0, \forall l$, implies a null column in the matrix G , thus a rank loss. Of course, if the anchors are not along the Y_w axis, the rank deficiency remains. This problem is avoided when the robot makes at least one turn. ■

Notice that the global observability is verified by means of (9), which can be used directly to design a filter. In fact, considering the presence of the noise in the ranging measurements (4), the actual problem to solve for offset estimation is a noisy version of relation (9)

$$h = 2G \begin{bmatrix} o_k \\ f_{x_k} \\ f_{y_k} \end{bmatrix} + g(\epsilon_k, \dots, \epsilon_{k+n}), \quad (10)$$

where the function $g(\cdot)$ account for all the uncertainties in the ranging measurements up to time $k+n$. Therefore, the localisation problem with unknown offset estimation amounts to computing the offsets using a Least Squares solution (or a Weighted Least Squares, if the stochastic description of $g(\cdot)$ are known) applied to (10) provided that the conditions in Theorem 2 are satisfied. If these conditions hold, the computed offsets can be subtracted away the offsets from the measured distances (4). As a consequence, it is possible

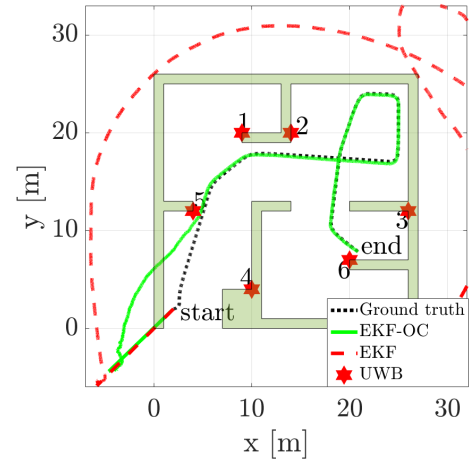


Fig. 1. Environment and the quality of trajectory estimation made by the standard EKF and EKF-OC in the first simulation scenario with the actual robot path (Dotted dark line) and the six UWB anchors (denoted with a number from 1 to 6).

to apply Theorem 1 concluding on the global observability of the trajectory. What is more, it is possible to feed the information on the offset into any filtering scheme (e.g., Extended Kalman Filtering), as shown below.

Remark 1 (real world observer design): The analysis above shows that there are strong theoretical basis to assert the observability of both the system state and the offset. The proof behind our results has a constructive nature and shows how an observer can be implemented to reconstruct state and offsets, provided that the following conditions hold:

- 1) The offset remains constant for at least three steps.
- 2) The measurements are not affected by noise.

In case any of these conditions is violated, we cannot guarantee convergence of the simple filter illustrated in the proof. However, the observability results pave the way for the application of more sophisticated filtering techniques such as EKF, which is illustrated in the following sections.

IV. SIMULATION RESULTS

The performance of the proposed approach to estimate the offset for localisation in indoor environments is firstly investigated through a series of simulations. In all scenarios, the robot is moving for 200 seconds following a predefined path in an environment equipped with 6 UWB anchors and with a constant linear velocity of $v = 0.3$ [m/s], while sampling both the wheels displacement and UWB ranging measurements with $T_s = 0.01$ seconds).

To show the practicality of the method, we first apply uncertainties into both the model and the UWB measurements which is considered to be normally distributed, zero-mean and white with $\sigma_\epsilon = 0.2$ [m], $\sigma_v = 0.15$ [m/s], and $\sigma_w = 0.1$ [rad/s]. We then assume a set of offsets, i.e. $o_k = 10$ [m], $\forall k \in [1, 6]$, which remains constant for a relatively long time during localisation. In order to show the efficacy of the proposed method, we propose here two possible design for an Extended Kalman Filter. The

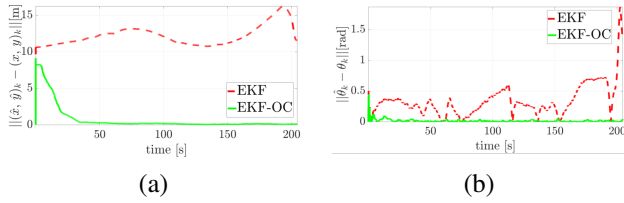


Fig. 2. Localisation error comparison between the standard EKF and EKF-OC, in presence of unknown offsets which remain constant for a relatively long time during localisation.

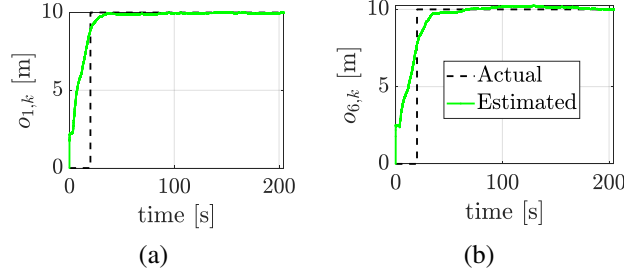


Fig. 3. Offset estimation performance for the EKF-OC solution with six UWB anchors with unknown offsets which remain constant for a relatively long time during localisation. Two different offsets are reported (the behaviour is similar the same for the others).

first one (named EKF) is a “standard” solution with three states (one for each kinematic variable). The second one (referred to as EKF-OC) has an additional state to account for the offset of each anchor (with null dynamics to model a constant variable). The results are compared in a qualitative and quantitative manner in Figure 1 and 2, respectively. In addition, Figure 3 reports the results of the offset estimation when the EKF-OC solution was applied. As can be seen from the figures, about 3 seconds after a change in the offset, it is correctly estimated. As a result, the EKF-OC scheme exhibits a largely superior performance.

In the second simulation scenario, we consider the NLOS conditions in a more realistic manner, where an unknown, time-varying offset is applying on the measurements. In particular, here we assume a normally distributed and zero mean uncertainty with the aforementioned characteristics is acting on both actuations and measurements. The major hurdle for the proposed EKF-OC is now to deal with a time varying offset induced by the robot motions and the environmental effects on the measurements. As reported in Figure 4 and Figure 5, for the same trajectory as the first simulation scenario, The EKF-OC delivers an acceptable accuracy in the estimation of the robot pose, whereas the standard EKF completely diverges. In addition, Figure 6 reports the accuracy of the offset estimation when the EKF-OC keeps track of the estimation of the time-varying offset in presence of a large measurement uncertainty.

The performance of EKF-OC appears to be acceptable recalling that, apart from a time varying offset, there is a large noise acting on both the actuation and measurements which has an additional detrimental effect. Since the proposed approach was conceived assuming a constant offset, this example shows that the effect of a time varying offset can

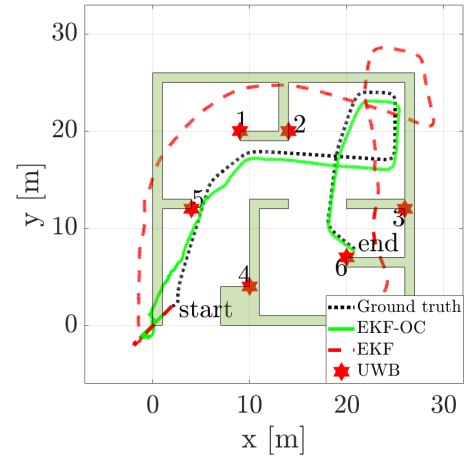


Fig. 4. Environment and the quality of trajectory estimation made by the standard EKF and EKF-OC in the second simulation scenario with the actual robot path (Dotted dark line) and the six UWB anchors (denoted with a number from 1 to 6).

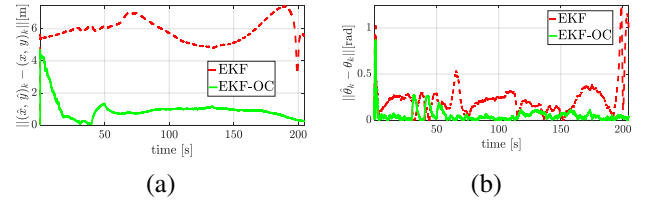


Fig. 5. Localisation error comparison between the standard EKF and EKF-OC, in presence of unknown, time-varying offset.

be managed with an adequate performance. What is even of major relevance, instead, is the effect that those estimated offset values have once applied in an EKF algorithm.

V. EXPERIMENTAL RESULTS

The effectiveness of the proposed method is further substantiated by the experiments conducted in the Department of Information Engineering and Computer Science (DISI) of the University of Trento (see Figure 7). The department is endowed with a localisation infrastructure (a testbed) consisting of a number of UWB anchors attached to the ceiling of the corridors and spaced 2.5 [m] apart. The anchors are DecaWave EVB1000 UWB nodes and are equipped with an STM32F105 MCU, a DW1000 UWB transceiver, and a PCB antenna. In the experimental setup, an additional UWB antenna (the emitter) is placed approximately on top of the robot inter axle. The robot ego-motion is measured also by two wheel encoders, which are sampled at 50 [Hz]. The estimated induced uncertainty in the model velocities are $\sigma_v = 0.1$ [m/s] and $\sigma_w = 0.06$ [rad/s]. Figure 7 shows the nominal trajectory followed by the robot along the long, narrow corridor. In the same figure, we also report the dead-reckoning results using the wheels relative encoders, which obviously drifts away from the nominal trajectory. The average linear velocity of the vehicle was $v = 0.5$ [m/s]. The distance between the UWB device on board of the robot and the anchors mounted on the ceiling was measured through a Single-Sided Two-Way Ranging (SS-TWR) scheme, which

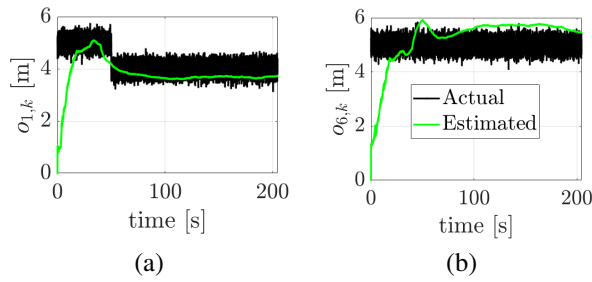


Fig. 6. Offset estimation performance for the EKF-OC solution with six UWB anchors with time-varying, unknown offset. Two different offsets are reported (the behaviour is similar for the others).

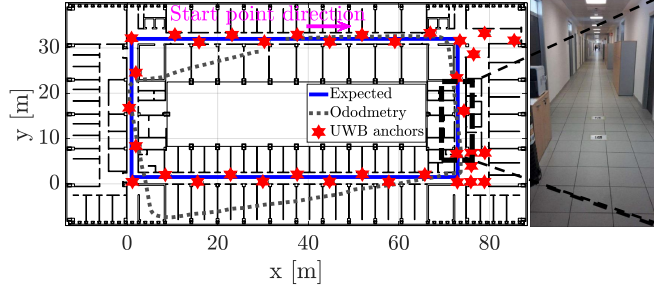


Fig. 7. Expected trajectory (think blue line) followed by the robot and the encoder-based dead-reckoning path (dotted black line) for the experimental validation, along with a snapshot of the long, narrow corridor (right inset). The red stars represents the UWB locations.

is based on the ToA measurements of a two-way message exchange. The distribution of the uncertainty effecting the UWB range measurements in LOS conditions is approximately Gaussian, with zero-mean and standard deviation $\sigma_r = 0.1$ [m]. The trajectory is particularly demanding for any localisation algorithm, because it is quite frequent that the visibility of a node is obstructed by a wall or by a locker (this is particularly true in the proximity of the corners of the trajectory). Moreover, due to the fact that the corridor is narrow and quite long, the UWB anchors are almost aligned, thus increasing the Geometric Dilution Of Precision (GDOP) of the ranging measurements and increase the uncertainty of trilateration and multilateration solutions. During the experiment, the fixed number of 4 measurements at each time step is considered for both filters, resulting in a state space representation with 7 states (i.e. robot pose and the TOA measurements vectors) for EKF-OC. The NLOS conditions are associated with an offset that jeopardises the correct operation of standard filters. This phenomenon can be easily observed by looking at the trajectory estimated by an EKF without offset compensation shown in Figure 8 (thick black line). As it is possible to see, the estimated robot pose is very frequently far way from the nominal trajectory, which runs in the middle of the corridor. For the EKF-OC however, as it can be seen from the figure, the proposed solution is able to localise the robot much closer to its actual trajectory. Indeed, the proposed EKF-OC technique delivers a much better result than a standard EKF, with the estimated trajectory remaining reasonably close to the actual one for most of the time. However, we can observe that even for the EKF-OC there

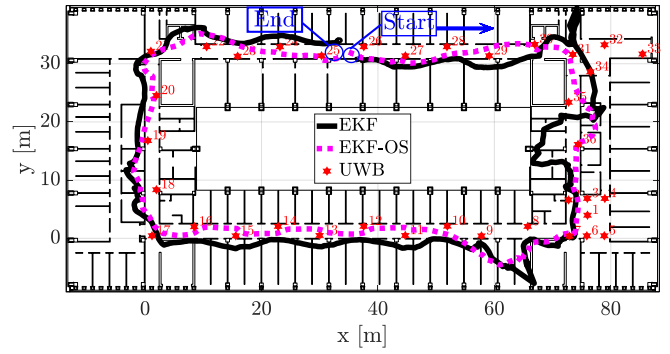


Fig. 8. Trajectory estimated by standard EKF and without offset estimation versus the trajectory estimated by the EKF with correcting offsets.

are areas of the building where the estimation error is quite large. Specifically, in the lower right corner of the map the combined effects of obstructions and reflections on the anchors from 1 to 7 produce a large deviation, which is difficult to recover. This is because the EKF takes some time to track the changes in the offsets of the different anchors and when there are many changes concentrated within a small space, we can have transient problems as shown in Figure 8. This consideration underscore the need for filter especially designed to manage this type of condition, which is one of the main direction of our future work.

VI. CONCLUSION

In this paper, we have addressed the problem of simultaneous estimation of the pose of a mobile robot and of the offsets in the distance from a set of UWB anchors that can be obstructed from the LOS of the robot. Our core result is a theorem that states under which conditions it is possible to reconstruct the state from a sequence of observations and, *at the same time*, estimate the offsets related to each anchor. Besides its theoretical significance, the result has a constructive form, meaning that it shows a linear system of equations that can be inverted producing the offsets using minimal number of anchors and observations. This method can be used as a module in a filtering scheme for state reconstruction, as shown by our experimental and simulation results.

Many points remain open for future investigation. The most important are to investigate the effect of the uncertainties in an analytic way, so as to compensate for them by design, and to study the performance of different observer and filtering schemes exploiting the techniques proposed in this paper.

REFERENCES

- [1] R. Siegwart and I. R. Nourbakhsh, *Introduction to Autonomous Mobile Robots*. Scituate, MA, USA: Bradford Company, 2004.
- [2] M. J. Gallant and J. A. Marshall, "Two-dimensional axis mapping using LiDAR," *IEEE Trans. on Robotics*, vol. 32, no. 1, pp. 150–160, Feb. 2016.
- [3] A. Davison, "Real-time simultaneous localisation and mapping with a single camera," 2003, pp. 1403–1410.

- [4] R. Mur-Artal and J. D. Tardós, "ORB-SLAM2: an open-source SLAM system for monocular, stereo, and RGB-D cameras," *IEEE Trans. Robotics*, vol. 33, no. 5, pp. 1255–1262, 2017. [Online]. Available: <https://doi.org/10.1109/TRO.2017.2705103>
- [5] D. Prokhorov, D. Zhukov, O. Barinova, A. Konushin, and A. Vorontsova, "Measuring robustness of visual SLAM," in *16th International Conference on Machine Vision Applications, MVA 2019, Tokyo, Japan, May 27-31, 2019*. IEEE, 2019, pp. 1–6. [Online]. Available: <https://doi.org/10.23919/MVA.2019.8758020>
- [6] B. Dzodzo, L. Han, X. Chen, H. Qian, and Y. Xu, "Realtime 2D code based localization for indoor robot navigation," in *Proc. IEEE Int. Conference on Robotics and Biomimetics (ROBIO)*, Shenzhen, China, Dec. 2013, pp. 486–492.
- [7] F. Zenatti, D. Fontanelli, L. Palopoli, D. Macii, and P. Nazemzadeh, "Optimal Placement of Passive Sensors for Robot Localisation," in *Proc. IEEE/RSJ International Conference on Intelligent Robots and System (IROS)*. Daejeon, South Korea: IEEE/RSJ, Oct. 2016, pp. 4586–4593.
- [8] V. Magnago, L. Palopoli, A. Buffi, B. Tellini, A. Motroni, P. Nepa, D. Macii, and D. Fontanelli, "Ranging-free UHF-RFID Robot Positioning through Phase Measurements of Passive Tags," *IEEE Trans. on Instrumentation and Measurement*, vol. 69, no. 5, pp. 2408–2418, May 2020.
- [9] D. Macii, A. Colombo, P. Pivato, and D. Fontanelli, "A Data Fusion Technique for Wireless Ranging Performance Improvement," *IEEE Trans. on Instrumentation and Measurement*, vol. 62, no. 1, pp. 27–37, Jan. 2013.
- [10] D. Giovanelli, E. Farella, D. Fontanelli, and D. Macii, "Bluetooth-based Indoor Positioning through ToF and RSSI Data Fusion," in *International Conference on Indoor Positioning and Indoor Navigation (IPIN)*. Nantes, France: IEEE, Sept. 2018, pp. 1–8.
- [11] K. Cheok, M. Radovnikovich, P. Vempaty, G. Hudas, J. Overholt, and P. Fleck, "UWB tracking of mobile robots," in *Proc. IEEE International Symposium on Personal Indoor and Mobile Radio Communications (PIMRC)*, Instambul, Turkey, Sep. 2010, pp. 2615–2620.
- [12] C. Zhang, M. J. Kuhn, B. C. Merkl, A. E. Fathy, and M. R. Mahfouz, "Real-time noncoherent uwb positioning radar with millimeter range accuracy: Theory and experiment," *IEEE Transactions on Microwave Theory and Techniques*, vol. 58, no. 1, pp. 9–20, 2010.
- [13] DecaWave, "DW1000 Data Sheet," 2016.
- [14] J. González, J. Blanco, C. Galindo, A. O. de Galisteo, J. Fernández-Madrigal, F. Moreno, and J. Martínez, "Mobile robot localization based on ultra-wide-band ranging: A particle filter approach," *Robotics and Autonomous Systems*, vol. 57, no. 5, pp. 496 – 507, 2009. [Online]. Available: <http://www.sciencedirect.com/science/article/pii/S0921889008001747>
- [15] A. Ledergerber, M. Hamer, and R. D'Andrea, "A robot self-localization system using one-way ultra-wideband communication," in *2015 IEEE/RSJ International Conference on Intelligent Robots and Systems (IROS)*, 2015, pp. 3131–3137.
- [16] V. Magnago, P. Corbalán, G. Picco, L. Palopoli, and D. Fontanelli, "Robot Localization via Odometry-assisted Ultra-wideband Ranging with Stochastic Guarantees," in *Proc. IEEE/RSJ International Conference on Intelligent Robots and System (IROS)*. Macao, China: IEEE, Nov. 2019, pp. 1607–1613.
- [17] A. Prorok, A. Arfire, A. Bahr, J. R. Farserotu, and A. Martinoli, "Indoor navigation research with the khepera iii mobile robot: An experimental baseline with a case-study on ultra-wideband positioning," in *2010 International Conference on Indoor Positioning and Indoor Navigation*, 2010, pp. 1–9.
- [18] L. Palopoli and D. Fontanelli, "Global Observability Analysis of a Nonholonomic Robot using Range Sensors," in *European Control Conference (ECC)*. Saint Petersburg, Russia: IFAC, May 2020, pp. 1300–1305, accepted.
- [19] L. Palopoli, D. Macii, and D. Fontanelli, "A Positioning Filter based on Uncertainty and Observability Analyses for Nonholonomic Robots," in *Proc. IEEE Int. Instrumentation and Measurement Technology Conference (I2MTC)*. Dubrovnik, Croatia: IEEE, May 2020, pp. 1–6.
- [20] A. Prorok, P. Tomé, and A. Martinoli, "Accommodation of nlos for ultra-wideband tdoa localization in single- and multi-robot systems," in *2011 International Conference on Indoor Positioning and Indoor Navigation*, 2011, pp. 1–9.
- [21] P. J. Rousseeuw, "Least median of squares regression," *Journal of the American statistical association*, vol. 79, no. 388, pp. 871–880, 1984.